Comparing the Performance of Two Gamma Cameras under High Counting Rates: Principles and Practice

Claus Guldberg and Niels Rossing

The Finsen Institute, Copenhagen, Denmark

The performance of two large Anger cameras at high counting rates was compared, and the principles for measuring the relevant parameters, especially deadtime loss and coincidence artifacts, are discussed.

The results demonstrate the importance of the following factors: modern pulse-shaping circuitry with short paralyzable deadtime, an anti-pileup circuit, and uniform energy information within the field of view, which requires separate summing matrices for energy and position.

Elaborate testing of the specifications should be carried out before purchase of a gamma camera.

J Nucl Med 19: 545–552, 1978

The performance of most—if not all—gamma cameras on the market is satisfactory for static imaging at low count rates. CT scanning, however, will reduce the need for such static studies, with bone scintigraphy as one of the few possible exceptions. In the future the main load will lie on dynamic functional studies. Many such procedures—in particular radiospirometry, radiocardiography and regional cerebral blood flow—demand such high count rates that the capabilities of the cameras become critical, and differences between their performances become evident (*1–4*). Currently, therefore, the performance at high count rates must be an essential criterion for the choice of a gamma camera.

The main objective of this study, accordingly, is to devise relevant methods of testing such performance in modern gamma cameras. The principles developed were applied to the testing of two large cameras: a) the LFOV of G. D. Searle (the "Searle camera") and b) the Maxicamera of General Electric (the "G.E. camera").

MATERIALS AND METHODS

The testing was concerned mainly with demonstrating the effects of deadtime loss and the coincidence phenomenon. We also studied the resolution and the geometrical distortion using a strong source in a scattering medium. Furthermore, we have investigated the position of the window in relation to the energy spectrum at various locations within the field of view, as well as the maximum window ranges.

Both cameras were interfaced with a computer system for flood-field calculations. The output count rates were taken from the scaler/timers of the two cameras. The Searle camera was tested only in short, unblank, high-countrate mode. Initially both cameras had been tested for gain shift* with increasing amounts of Tc-99m activity evenly mixed in a water flood field 12 cm thick to ensure that the pulse load to all 37 PM tubes would be equal under most clinical situations. In these conditions both cameras showed only a minimal gain shift between 100 and 100,000 cps output as measured with a 30% window.

The following methods were then used to determine the wanted parameters:

1. The deadtime loss for Tc-99m in a scattering medium was determined by measuring the physical decay of the nuclide in a water flood field, 12 cm thick, over a period of 72 hr. The window was 30% and set before the study at a count rate of about 100 cps. The fraction of the spectrum within the

Received Sept. 26, 1977; revision accepted Dec. 29, 1977.

For reprints contact: Claus Guldberg, Dept. of Clinical Physiology, The Finsen Institute, Strandboulevarden 49, DK-2100 Copenhagen Ø.

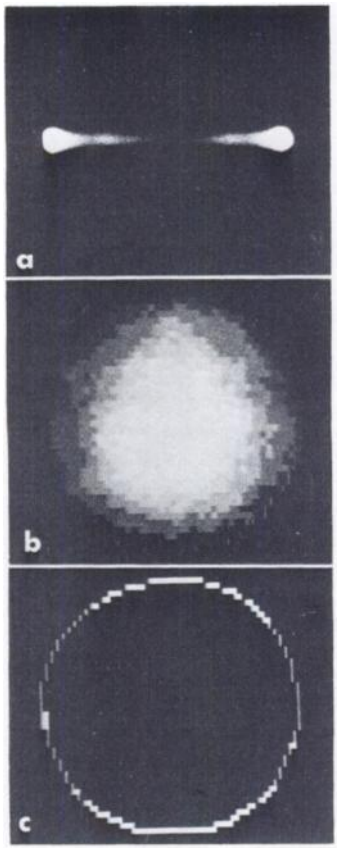

FIG. 1. (a) Coincidence errors in G.E. camera between two Tc-99m point sources, with 10 cm of water to provide a scattering medium. (b) Tc-99m flood-field image from G.E. camera with distortion due to coincidences. There is an accumulation of pileup artifacts at the center. (c) Peripheral zone shows no pileup artifacts, even at high count rates.

window averaged 41% for the total field of view. The output count rate in the window decreased during the measurement from about 100,000 cps to about 100 cps.

2. The coincidences in the two cameras were measured as a function of input count rate to a 30% window. The window was initially set over the 141-keV peak to give the maximal count rate from a low-activity Tc-99m flood field of 50 × 50 × 12 cm filled with water as a scatter medium to mimic a clinical situation with respect to Compton scatter and coincidences. For the Searle camera the measurement was repeated with the window set at a high count rate (about 95 kcps output through the window from a high-activity flood field). With increasing amounts of Tc-99m, a series of flood fields were recorded with an increasing percentage of coincidences. To separate the coincidences in the window from the peak and the scatter counts in the same window we took advantage of the fact that the coincidences between two sources in the field of view are projected on a line between them (Fig. 1). Consequently, in a homogenous flood field—which may be considered as consisting of concentric cylinders—coincidences will concentrate in the center and decrease toward the periphery (Fig. 4 shows an example). Although the input ratio between Compton scatter and the total number of counts from a flood field will be highest at the center, it will not change as a function of the count rate.

Therefore, the coincidence artifacts in the window from each high-activity flood field was determined as the difference between this image and an image of a field of low intensity, where there are very few coincidences. The latter flood field must contain the same number of counts in the peripheral zone as in the same peripheral, coincidence-free zone of the high-intensity flood field (Fig. 2).

Naturally, the ratio of Compton scatter over total counts anywhere in the field of view is nearly independent of the sensitivity of the parallel-hole collimator, a fact easily demonstrated experimentally. Thus, the different sensitivities of the three collimators used in the study do not influence the theoretical calculations.

3. The resolution of an Anger camera cannot be defined at high count rates by FWHM and MTF values because of the additional degradation due to coincidences. Therefore, we used a string phantom of 1.2-mm Teflon® tubing (0.7-mm lumen), filled with about 250 mCi Tc-99m and placed 10 cm from the collimator surface in a water bath 20 cm deep. The window was 30%. Each recording contained 10 million counts to minimize the influence of random regional variation. In these cases also, the fraction of the spectrum within the window was 41%.

With the General Electric "low-energy, high-resolution" parallel-hole (LEHR) collimator, the recording was performed with about 100,000 cps

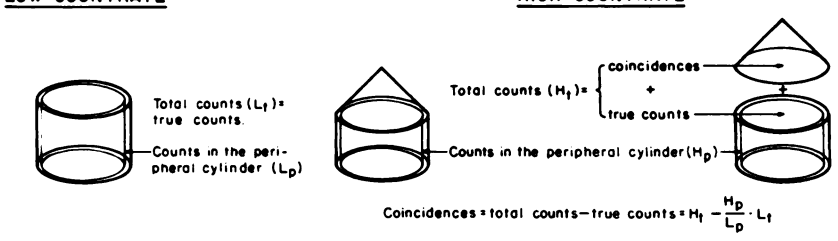

FIG. 2. Quantitative calculation of pileup distortion with a high-activity flood field. Pulses distorted by pileup are separated from (Compton) scatter and nonscatter pulses by subtraction of a low-activity flood field. Both flood fields contain same number of counts in coincidence-free peripheral zone (see text).

at the window output. The sensitivity of the collimator was determined with a Co-50 phantom, that yielded a count rate of 3,200 cps from a 30% window placed over the 122-keV peak.

The Searle "low-energy all-purpose" parallel-hole (LEAP) collimator was similarly found to have a sensitivity corresponding to 4,000 cps. The Searle "high-resolution parallel-hole" (HRPH) collimator was tested at 68,000 cps output and was found to have a sensitivity corresponding to a 2,800 cps output with the Co-57 phantom.

4. Additional measurements of Tc-99m spectra in air and water, at low and high count rates, were performed with the Searle camera using a 5% relative window and converting the count rate obtained to that from a fixed window. The measurements in air were done with the Tc-99m in only 0.4 ml water placed at the focus of a converging collimator. The measurements in water were performed with the Tc-99m water flood field 12 cm thick.

All the spectra were recorded with slightly increased high voltage to the PM tubes to extend the low end of the spectrum from the normal lower limit of 50 keV down to 18 keV. This was necessary to obtain a reliable estimate of the dual-coincidence spectrum in water.

The anti-pileup circuit in the Searle camera has an opening time of about 100–200 nsec, which results in minimal phase shift between the coinciding pulses. Thus, it is valid to equate the keV value of a pileup pulse with the sum of the keV values of the coincident pulses. The probability of two pulses coinciding is proportional to the product of probabilities of each of the individual pulses. The probability of a dual coincidence with a given keV value, E, will thus be the sum of the probabilities of all dual coincidences with this sum energy—i.e., the integral from 0 to E of f(X) multiplied by f(E − X), where f(X) and f(E − X) are the probabilities obtained from the low-count-rate spectra of pulses with energies of X and E − X, respectively. Accordingly, the theoretical dual-coincidence spectra were calculated from the low-count-rate spectra in air and water by means of a convolution integral as illustrated in Fig. 7b and e (*8,9*).

5. The window setting of the Searle camera was the same anywhere in the field of view, due to the separate summing matrices for the energy and position pulses from the preamplifiers. There is no such separation in the G.E. camera, so for this camera a quantitative estimate of the various peak settings in the field of view was performed in the following manner. With a Tc-99m flood field of low intensity (to avoid coincidences), the common high-voltage control of the PM tubes was adjusted to yield maximum output count rate with a 5% window. With equidistant changes in high voltage—5 steps up and 5 steps down—a total of 11 flood fields were recorded from 122 keV (checked with a Co-57 source) to 159 keV (checked with an I-123 source). After correction for recording time and decay of the Tc-99m source during the period of measurement, the regional differences between the individual flood fields were used to calculate the keV values of the regional window centerlines in the field of view.

RESULTS

Deadtime loss and coincidences. Figure 3 shows the output count rate as a function of input count rate in the G.E. camera (a) and in the Searle camera with the window set at low (b) and high (c) count rates. Both cameras have almost the same total output curves, but they contain highly different calculated numbers of coincidences. Consequently, the true output curves, obtained by subtracting the coin-

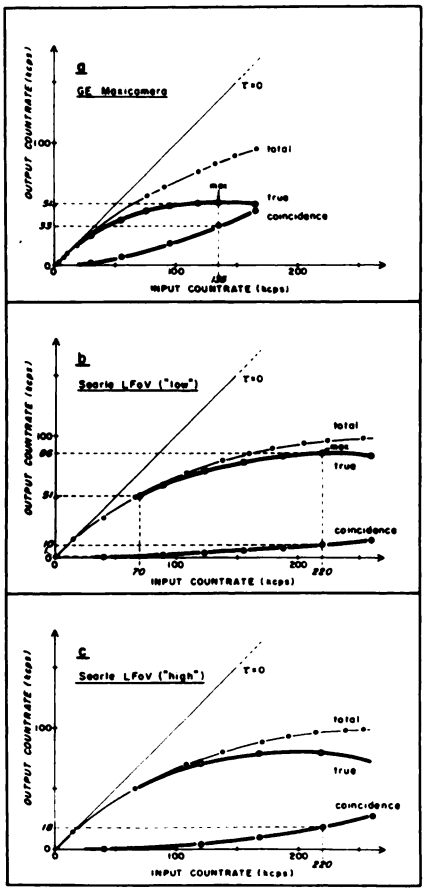

FIG. 3. (a) Output and coincidence count rates in G.E. camera's 30% window as functions of input count rate from a 12-cm-high water-filled Tc-99m flood field. Window was calibrated at low count rate; fraction of integral input count rate in window = 41%. (b) Output and coincidence count rates in Searle camera. Measuring conditions as in (a). (c) As in (b), except that the window was calibrated at maximum output count rate. Note consequent increase in coincidence count rate.

cidences from the total counts, are significantly different for the two cameras. For the G.E., maximum true output was 51 kcps plus 33 kcps from coincidences at an input countrate of 135 kcps. The corresponding figures for the Searle camera were 86 kcps as a maximum true output, with an addition of 10,000 coincidence cps at an input of 220 kcps. A true output of 51 kcps is obtained with the Searle camera with only 1,000 coincidence cps at an input countrate of 70 kcps (Fig. 3b). Figure 3c shows about 80% increase in coincidences due to the setting of the window at a high count rate. Figure 4 illustrates the image distortion in the G.E. camera due to pileup. In contrast, Fig. 5 shows the beneficial effect of the Searle anti-pileup circuit.

Resolution. Figure 6 shows how the coincidences at high count rates degrade the resolution. The tube phantom was placed in the middle of a 20-cm-deep water bath, 10 cm from the collimator surface. At a total output of about 100 kcps in the window, the G.E. camera had a resolution of 14 mm, with obvious spatial distortion at the periphery. The Searle camera, with a LEAP collimator, had a resolution of 12 mm and no detectable spatial distortion. The best resolution (11 mm) was obtained with the Searle HRPH collimator at a total window output of 70 kcps.

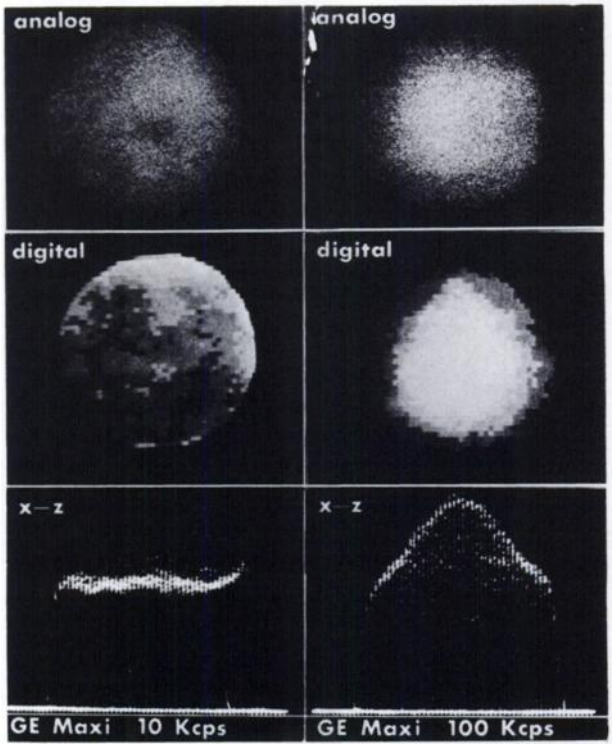

FIG. 4. Effects of low- and high-activity flood fields on G.E. camera in analog, digital (64 × 64), and X-Z display. Recording conditions: 12-cm-high water-filled Tc-99m flood field; window = 30%, which accepts 41% of input spectrum.

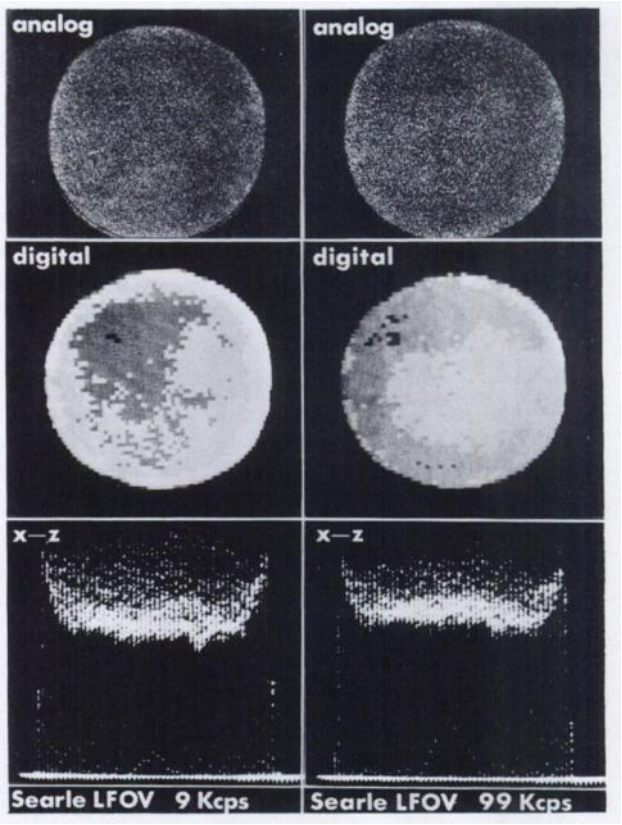

FIG. 5. Effects of low- and high-activity flood fields on Searle camera, under same conditions as in Fig. 4. Note minimal distortion in high count-rate flood field.

Spectral analysis. The spectra determined with the Searle camera in air and water at low and high count rates are shown in Fig. 7a, c, d, and f, together with spectra of dual coincidences (Fig. 7b and e) as calculated by convolution of the low-count-rate spectra (Fig. 7a and d). The Compton scatter in water at low count rate is taken as the difference between the spectra obtained in water (Fig. 7d) and air (Fig. 7a). the coincidences above and within the window are estimated by comparing the spectra of Fig. 7f with Fig. 7d and e. A 30% window, set symmetrically over 141 keV, is inserted in Figs. 7d, e, and f in order to show the distribution of Compton scatter and coincidences within the window.

Energy uniformity. Figure 8 shows that when a G.E. camera with a 30% window is adjusted to maximum output count rate from a Tc-99m flood field, the midline of the window corresponds to 122 keV in the center of the field and moves up to 159 keV at the periphery.

Table 1 summarizes the most important features of the two cameras. Measured and advertised data are compared.

DISCUSSION

There is an abundant literature on the deadtime

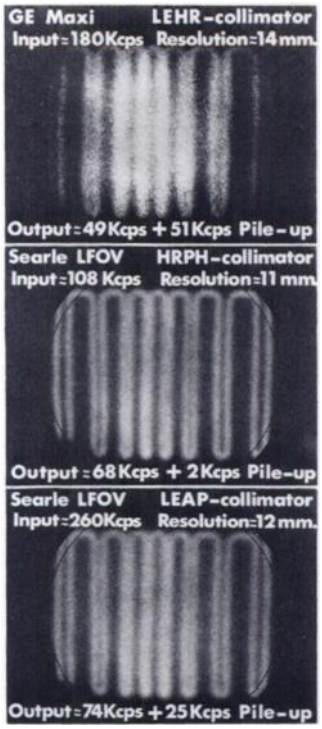

FIG. 6. Resolution of the two cameras at high count rates, measured with a string phantom with 250 mCi Tc-99m placed 10 cm from collimator surface in a 20-cm-deep water bath to provide scatter. Internal diameter of tube = 0.7 mm; line separations from left to right: 18, 14, 10, 8, 9, 12, 16, and 20 mm. All count rates refer to 30% window calibated at low count rate, accepting 41% of integral input counts.

problems in gamma cameras, and the pileup artifacts have also been known for several years (*10*). From a technical point of view it has been possible for at least 10 yr to meet the demands that high input flexes impose on gamma cameras by using principles established in nuclear spectroscopy (*11*).

Deadtime loss and pileup measurements. Although Compton scatter is independent of count rate and will only cause decrease in contrast and resolution, this is not so with coincidences. Their number will increase rapidly with the count rate. Furthermore, in the clinical situation both their amount and position are unpredictable and cannot be corrected for, since in the field of view they become displaced in relation to the coincident scintillations. Their number also depends on the varying regional spectral distortion due to Compton scatter.

From the flood field, the G.E. camera had a maximal true output of 51 kcps in a 30% window, corresponding to an integral output of 125 kcps. If the mean coincidence error in the window must not exceed an arbitrary value of 5%, the camera tested will not be satisfactory with an output of more than 25 kcps (Fig. 3a).

The Searle camera, on the other hand, had a maximal true output of 86 kcps in the 30% window, corresponding to an integral output of 212 kcps. This is only an approximation, because in the Searle camera the deadtime after pulses within the window is somewhat longer than after pulses outside the window. The correct value is close to 200 kcps. The camera performs adequately with a maximum of 5% coincidences in the window at an output of 70 kcps (Fig. 3b) in the measurement situation chosen to imitate a "worst case" clinical situation with respect to Compton scatter and coincidences. The reason why Murphy et al. (*4*) obtained somewhat different results is that they performed their measurements in air†, thus providing almost no scatter and generating only negligible probability for coincidences in the window. This can be seen in Fig. 7b and c.

Note that the procedure used to separate nonscattered pulses and Compton scatter from the pileup artifacts is necessary for a valid comparison of the cameras. A simple registration of the total number of counts in the area showing pileup artifacts between two or more sources would also include Compton scatter, blurring the result. One of the cameras (the G.E.) did not have a separate summing matrix. This necessitates detuning of the PM tubes, which causes different window settings (Fig. 8) and therefore the amounts of admixed Compton scatter within the field of view are different for the two cameras. This not only makes a comparison impossible, but also generates artifacts by flood-field correction on the G.E. camera (*12*).

Spectrum analysis. The calculated dual-coincidence spectra were in excellent agreement with the spectra measured at higher count rates (Fig. 7). Figure 7f demonstrates that an optimal setting of the window involves a risky voyage between the scatter at the lower level and the coincidences at the upper level. Success depends on an identical spectral window setting anywhere within the field of view. This requires electronic separation of the energy and position pulses from the preamplifiers that follow the PM tubes, which is the case in the Searle camera but not in the G.E. Maxicamera (Fig. 8).

Figure 7, e and f, illustrates an important phenomenon: with the coincidences placed around and above the upper level of the window, and with their rapid increase in number with increasing count rate, a window set for maximal output in a high-count-rate calibration will necessarily be set higher in the spectrum than if the setting had been performed at a low count rate. This phenomenon, of course, has nothing to do with gain shift. Therefore, automatic or manual window setting for maximum output count rate during dynamic investigations with changing count rates should be avoided, since this would result in a marked increase in coincidence errors at high

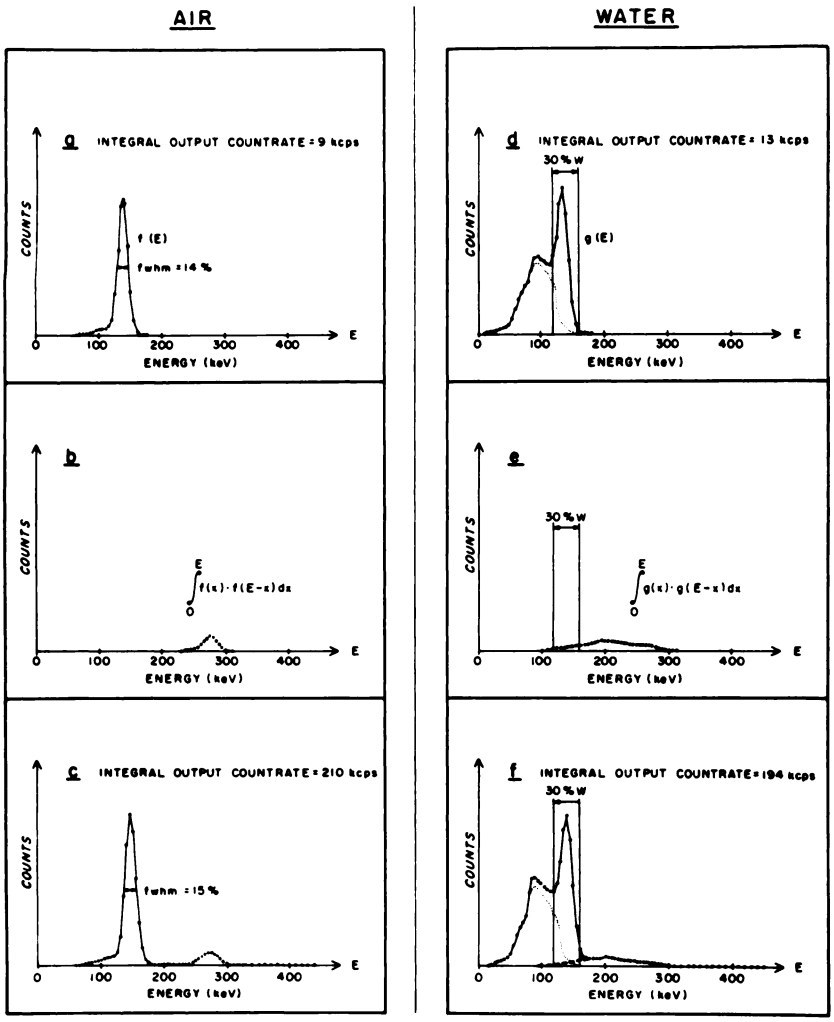

FIG. 7. Technetium-99m spectra recorded Searle camera at low and high count rates, with and without scatter medium. Also dual-coincidence spectra as calculated from low-count-rate spectra by means of a convolution integral. Note in (a) that there are no detectable x-rays from lead in the collimator, and in (c) that triple coincidences are negligible.

count rates. This is verified by the experiment of Fig. 3c, which shows an extra coincidence measurement with the Searle camera, the window being set for maximal output at a high count rate. Comparison with Fig. 3b shows that the coincidence error at the same input count rate has now increased 80%. Consequently, the window calibration must be performed at low count rates, and a still lower setting may be necessary, tolerating a higher scatter contribution. In a previous work (*13*) we have shown that when the nuclide is Xe-133—as will typically be the case in radiospirometry and cerebral blood-flow measurements—this Compton scatter in the window may easily be cut in half by a 1-mm brass filter between the collimator and the NaI crystal. At the same time a filter of this type for Xe-133 in water will cause a marked reduction in the number of coincidences in the window.

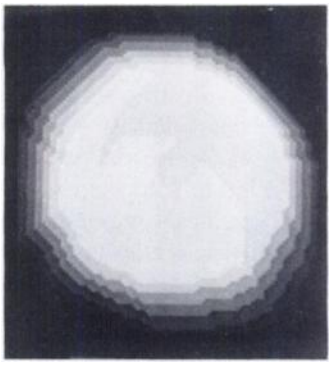

FIG. 8. Variations of effective window position within field of view of G.E. camera (see text). Window settings vary from about 160 keV at periphery to about 120 keV at center, with a mean value of 141 keV for the whole field of view. Each grey-shade step corresponds to an energy interval of 5 keV.

The lack of an anti-pileup circuit in the G.E. camera tested (and in other cameras as well) does give rise to a noticeable increase of coincidences. Their indicated energy will be less than the sum of the pulses from the coinciding scintillations. This is due to the greater phase shift between the electronic pulses that coincide, which allows the peak of one pulse to coincide with the tail of another. The total coincidence spectrum, therefore, will be shifted

TABLE 1. COMPARISON OF SEARLE LFOV AND GENERAL ELECTRIC MAXICAMERA (1976)

	Maximum true integral output count rate in kcps advertised/ measured	Maximum true output count rate within a 30% window + additional coincidences in kcps	Resolution in mm at a distance of 10 cm advertised/ measured	Visible geometric distortion	Number of windows/wide range window from 50 to 600 keV	Uniform energy information within field of view
G.E. maxicamera	200/125	51 + 33	10/14	yes	1/no	no
Searle LFOV	200/200	86 + 10	11/11	no	3/yes	yes
		(51 + 1)	12/12			

downwards, and the extra coincidences within the window will be more evenly distributed from the lower to the upper level. This, of course, is the reason why the pseudo-gain-shift described earlier cannot be observed in the G.E. camera in spite of the far greater number of coincidences. This construction does not permit a reduction of coincidences by a lower window setting.

Maximum useful output count rate. Even after subtraction of coincidences, the maximal output count rate provides no reliable guide to the useful count rate in a given clinical study. At maximum output count rate, small variations in photon flux will cause no change in the output. Thus, there is a "no-response region." For a system with a simple paralyzable deadtime, it can be shown that even at a deadtime loss of 27%, a 1% change in the input count rate will change the output countrate by no more than 0.5%. The corresponding figures at 50% deadtime loss are 1% and 0.15%, respectively. Even if these reduced changes are still recorded as statistically significant for the whole field of view, this will be difficult or even impossible regionally, where the counting statistics are worse due to the fewer counts and the hypergeometric uncertainty of distribution of counts in the field of view (*13*). A maximal loss of differential sensitivity of 50% to changes in the input countrate (= changes in activity), corresponding to a paralyzable deadtime loss of about 27%, represents another reasonable upper limit for the suitability of an Anger camera for quantitative clinical studies. In the described recording situation—30% window and a 12-cm-thick flood field—this corresponds to a maximum output of 36 kcps for the G.E. camera and 55 kcps for the Searle. To comply with the arbitrary requirement of an average maximum of 5% coincidences in the field of view, the G.E. camera will have an upper limit of 25 kcps and the Searle camera one of 55 kcps.

Resolution measurements. The resolution measurements under "worst case" conditions (Fig. 6) illustrate the importance of an anti-pileup circuit and modern pulse handling. Even at a higher input count rate and with a more sensitive collimator, the resolution is 2 mm better in the Searle camera than in the G.E. The best resolution is obtained with the Searle camera and a high-resolution collimator. Because of the lower input countrate, compared with the LEAP collimator, the pileup artifacts are markedly reduced, whereas at the same time the output count rate is only slightly decreased, due to the smaller deadtime losses. In spite of the lower input count rate, the output count rate remains higher than with the G.E. camera. Note that there is no visible geometrical distortion in the Searle images of Fig. 6, b and c, whereas this is present in the periphery of the G.E. image (Fig. 7a), possibly as a result of the absence of a light guide in the G.E. camera.

FOOTNOTES

* Gain shift is changing gain of the PM tubes with increasing count rate, mainly due to heating of the last dynodes and poor stabilization in their voltage supply.

† Personal communication.

REFERENCES

1. LANGE D, KOBER B, SCHENCK P, et al: Totzeitverluste und Pile-up bei hohen Zählraten in Szintillationskameras. *Radioaktive Isotope in Klinik und Forschung*. Vienna, H. Egermann, 1976, 12: pp 557–568

2. LANGE D, HERMANN HJ: Zur Bedeutung der Korrekturen von Gammakamerabilder bei hohen Präparatsstärken. *Compact News in Nucl Med* 113–116, Okt. 1976

3. LANGE D, HERMANN HJ, WETZEL E, et al: Critical parameters to estimate the use of a scintillation camera in high dose dynamic studies. In *Medical Radionuclide Imaging*. Proceedings of a Symposium, Los Angeles, Oct. 1976, IAEA, Vienna 1977, pp 85–97

4. MURPHY P, ARSENEAU R, MAXON E, et al: Clinical significance of scintillation camera electronics capable of high processing rates. *J Nucl Med* 18: 175–179, 1977

5. BOSNJAKOVIC VB, BENNETT LR, GREENFIELD LD, et al: Dual-isotope method for diagnosis of intracardiac shunts. *J Nucl Med* 14: 514–521, 1973

6. BLOCH P, SANDERS T: Reduction of the effects of scattered radiation on a sodium iodide imaging system. *J Nucl Med* 14: 67–72, 1973

7. WELLMAN HN, KEREIAKES JG, YEAGER TB, et al: A

sensitive technique for measuring thyroidal uptake of iodine-131. *J Nucl Med* 8: 86–96, 1967

8. WAIBEL E: Zur Berechnung von Pile-up-Spektren. *Nucl Instr and Meth* 74: 236–244, 1969

9. WAIBEL E: Bestimmung der Faltungsfunktion zur Berechnung von Spektren aufgestockter Impulse. *Nucl Instr and Meth* 86:: 29–34, 1970

10. DRATZ AF: Stationary imaging devices. In *Continuing Education Lectures*, New York, Society of Nuclear Medicine, 1971, chapter 7

11. BLATT SL, MAHIEUX J, KOHLER D: Elimination of pulse pileup distortion in nuclear radiation spectra. *Nucl Instr and Meth* 60: 221–230, 1968

12. PADIKAL TN, ASHARE AB, KEREIAKES JG: Field flood uniformity correction: Benefits or pitfalls? *J Nucl Med* 17: 653–656, 1976

13. GULDBERG C, KARLE A, BALSLEV-JØRGENSEN P: Anger camera imaging of perfused and non-perfused brain tissue with the intraarterial ^{133}Xe-method. *Europ J Nucl Med*: in press